Standardized Evaluation of Chemical Compositions of $LiTaO_3$ Single Crystals for SAW Devices Using the LFB Ultrasonic Material Characterization System

Jun-ichi Kushibiki, *Member, IEEE*, Yuji Ohashi, and Takaaki Ujiie

Abstract—**The line-focus-beam ultrasonic material characterization (LFB-UMC) system is applied to compare and evaluate tolerances provided independently for the Curie temperature T_C and lattice constant a to evaluate commercial $LiTaO_3$ single crystals by measuring the Rayleigh-type leaky surface acoustic wave (LSAW) velocities V_{LSAW}. The relationships between V_{LSAW}, and T_C and a measured by individual manufacturers were obtained experimentally using $42°YX$-$LiTaO_3$ wafers as specimens from three crystal manufacturers. In addition, the relationship between V_{LSAW} and SH-type SAW velocities V_{SAW} that are actually used for the SAW device wafers was obtained through calculations, using the chemical composition dependences of the acoustical physical constants for $LiTaO_3$ crystals reported previously. The result of a comparison between the T_C tolerance of $\pm 3°C$ and the a tolerance of ± 0.00002 nm through the common scale of V_{LSAW} or V_{SAW} demonstrated that the a tolerance is 1.6 times larger than the T_C tolerance. Furthermore, we performed a standardized comparison of statistical data of T_C and a for $LiTaO_3$ crystals grown by two manufacturers during 1999 and 2000, using V_{LSAW}. The results clarified the differences of the average chemical compositions and of the chemical composition distributions among the crystal ingots between the two manufacturers. A guideline for the standardized evaluation procedure has been established for the SAW-device wafer specifications by the LFB-UMC system.**

I. Introduction

The rapid spread of mobile communications on a global scale in recent years has increased the demand for surface acoustic wave (SAW) devices used for these communications systems [1]–[3]. As the performance of SAW devices depends not only on the device fabrication processes but also on the homogeneity of the chemical and physical characteristics of the substrate materials themselves, production of single crystals highly homogeneous in chemical composition is very important from the technological point of view. Furthermore, it is necessary to develop large-diameter, high-quality crystals to meet the requirements for SAW devices, such as compactness, higher-frequency operation, and low cost. It is also important to develop a new method for evaluating their elastic homogeneity.

In present industries, the chemical compositions of $LiTaO_3$ and $LiNbO_3$ single crystals are evaluated mainly using the Curie temperature T_C, which is measured by thermal analysis methods such as differential thermal analysis (DTA) and differential scanning calorimetry (DSC). Some manufacturers use the lattice constant a measured by X-ray diffractometry for evaluation. Controlling the chemical composition ratio is difficult, and some variations in chemical composition ratio can occur, even in crystals grown by a single manufacturer, due to slight fluctuations in the growth conditions. Therefore, it is necessary to select or evaluate grown crystals by measuring T_C or a to obtain substrates with the required characteristics. However, the relationship between T_C and a and the interrelationships among these and the SAW velocities V_{SAW} have not yet been clarified; and at present, measurement errors in each evaluation approach as well as the tolerances in the evaluated results differ from one manufacturer to another. For that reason, the property distributions in and among substrates that are supplied vary from one manufacturer to another, and users must consider this to be a primary cause for the lowered yield in the fabrication of devices. It is important to clarify the relationships among the chemical and physical characteristics, such as the chemical composition, T_C, a, and V_{SAW}, and to compare and review the tolerances for various characteristic values under standardized specifications.

We have been studying the development and application of a highly precise material characterization technology incorporated in the line-focus-beam ultrasonic material characterization (LFB-UMC) system [4], [5]. We have so far achieved various results, mainly for $LiNbO_3$ and $LiTaO_3$ single crystals [6]–[14]. Specifically, we evaluated 127.86° rotated Y-cut X-propagating $(128°YX)$-$LiNbO_3$ [15] and X-cut 112.2° rotated Y-propagating $(X-112°\ Y)$-$LiTaO_3$ [16] wafer substrates that are widely used for SAW devices. These evaluations identified, with great accuracy, some variations caused by the chemical composition ratio changes and some serious problems in the poling process as the changes of leaky surface acoustic wave (LSAW) velocities V_{LSAW} [7], [14]. However, the variations of V_{LSAW} due to the chemical composition changes depend on the surface

Manuscript received September 14, 2001; accepted November 8, 2001. This work was supported in part by Research Grants-in-Aid from the Ministry of Education, Science, and Culture of Japan and from the Japan Society for the Promotion of Science for the Research for the Future Program.

The authors are with the Department of Electrical Engineering, Tohoku University, Sendai 980-8579, Japan (e-mail: kushi@ecei.tohoku.ac.jp).

orientation and wave propagation direction. Therefore, it has been necessary to experimentally obtain the relationships (calibration lines) between the chemical composition ratios and V_{LSAW} for required surface orientations and propagation directions [8]–[11], [13], [14]. It is important to determine the elastic homogeneities as V_{SAW} variations to evaluate materials for SAW devices. Measurements in the LFB-UMC system are performed with water loaded on the surface of the specimen from its principle of operation. Therefore, the V_{SAW} of the propagation mode (particularly the SH type [17]) actually used in SAW devices cannot be evaluated directly using Rayleigh-type LSAWs efficiently excited on the surface [10]. V_{SAW} for the desired surface specimens and propagation directions has been measured conventionally by adopting a common method of forming interdigital transducers (IDTs) [18], [19] on the substrates. However, this method is not the best one for evaluation because it is time consuming to fabricate IDTs, it is not suitable for two-dimensional inspection on the substrate, and it cannot exclude the additional variations introduced through the IDT fabrication process when attempting to obtain the intrinsic acoustic characteristic variations of the substrate itself.

We recently determined the chemical composition dependences of the acoustical physical constants for $LiNbO_3$ and $LiTaO_3$ single crystals [20]. This enables us to obtain the chemical composition dependences of V_{LSAW} and V_{SAW} for an arbitrary surface orientation and propagation direction by numerical calculations. It also enables us to obtain the relationship of V_{LSAW} or V_{SAW} with the chemical composition ratios. Therefore, by converting the Rayleigh-type V_{LSAW} variations, measured by the LFB-UMC system, into V_{SAW} variations, we can evaluate both Rayleigh-type SAW device materials and SH-type SAW device materials properly.

To evaluate the chemical composition of $LiTaO_3$ single crystals in this study, we attempt a standardized comparison and evaluation of the tolerances of T_C and a, independently provided by individual manufacturers, by means of the Rayleigh-type V_{LSAW}, measured using the LFB-UMC system. SH-type 42° rotated Y-cut X-propagating $(42°YX)$-$LiTaO_3$ single crystal wafer substrates [21], [22] were adopted for demonstration.

II. Relationship Between LSAW and SAW Velocities

We recently reported on the chemical composition dependences of the acoustical physical constants (elastic constant, piezoelectric constant, dielectric constant, and density) for $LiNbO_3$ and $LiTaO_3$ single crystals [20]. This information enables us to obtain the chemical composition dependences of acoustic properties for an arbitrary surface orientation and propagation direction through theoretical calculations. It also enables us to estimate the changes in SH-type V_{SAW} by calculations from the experimentally obtained changes in Rayleigh-type V_{LSAW}. We apply this method to $42°YX$-$LiTaO_3$ wafer substrates for SH-type SAW devices.

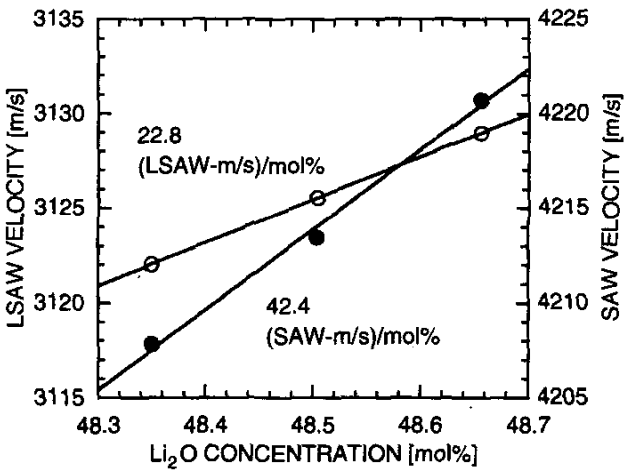

Fig. 1. Calculated Li_2O concentration dependences of LSAW and SAW velocities for $42°YX$-$LiTaO_3$ single crystals. Circles: LSAW, dots: SAW, solid lines: approximated lines obtained by the least-squares fitting to each set of the calculated data.

Fig. 1 shows the calculated results of the chemical composition dependences of Rayleigh-type V_{LSAW} as circles and SH-type V_{SAW} as dots for $42°YX$-$LiTaO_3$ wafers. The numerical calculations were conducted according to the methods in the literature [23] for LSAW and [24] for SAW using the constants reported in the literature [20]. The straight lines are the approximated lines obtained by the least-squares fitting to each set of the calculated data. The calculated values of V_{LSAW} and V_{SAW} tend to increase linearly as the Li_2O content $M(Li_2O)$ increases, and the relationships of V_{LSAW} and V_{SAW} to $M(Li_2O)$ are obtained as 22.8 (LSAW-m/s)/mol% and 42.4 (SAW-m/s)/mol% from the gradients of the approximated straight lines. We here use the unit expressions of LSAW-m/s and SAW-m/s to discriminate V_{LSAW} from V_{SAW}. A comparison between V_{LSAW} and V_{SAW} reveals that V_{SAW} has a greater dependence on the changes in chemical composition ratio. This result is closely related to the fact that, although the components of the acoustical physical constants associated with the SH-type V_{SAW} are the same as those associated with the Rayleigh-type V_{LSAW}, they contribute differently to the two velocities because of the different mode conditions, resulting in the very large electromechanical coupling factor for the SH-type SAW and almost zero for the Rayleigh-type SAW and LSAW [10], [17], [23], [24]. From the results shown in Fig. 1, we can obtain the relationship between V_{LSAW} and V_{SAW}, i.e., the ratio of the SH-type V_{SAW} to V_{LSAW} around the congruent composition, as 1.85. This enables us to obtain V_{SAW} theoretically by measuring V_{LSAW} with the LFB-UMC system.

III. LFB-UMC System

The measurement principle of the LFB-UMC system was presented in detail in the literature [4]. The LSAW propagation characteristics (viz., phase velocity and attenuation) can be obtained by measuring and analyzing the transducer output of $V(z)$ curve, obtained as a function of the relative distance z between the LFB ultrasonic device and the specimen. Errors in the movement of the mechanical translation z stage and in the measurement of the temperature of the water used as the coupling material between the ultrasonic device and the specimen are the primary error factors for LSAW velocity measurements. We have developed a newer system [5] to minimize the errors in measurements of the couplant temperature by installing the whole mechanical system, including the ultrasonic device and specimen, in a temperature-controlled chamber to stabilize the temperature environment.

The system used at this time is the newest system and achieves the highest accuracy among the LFB-UMC systems that we have developed. In the previous system, we accurately measured the translation distance using a laser interferometer by adopting a stage of an air-bearing system with superior straightness of translation for the z stage [5]. In contrast, we used a ball-bearing system for the z stage in the newest system, and gave sufficient rigidity to the z stage and the support to fasten the z stage. We measured the relative phase changes of the signals reflected from the reflector as a function of the distance z to compare the translation characteristics between the two stages, using a technique that employs a plane wave ultrasonic device operating at 200 MHz [25]. Fig. 2 shows the results obtained by subtracting the phase changes due to propagation of longitudinal waves in water from the measured phases. The results in Fig. 2(a) exhibit a constant phase variation width of $\pm 2°$ around relative phase zero regardless of the position of z. In contrast, the results in Fig. 2(b) present different characteristics, depending on the position of z, with relatively large undulations of changes in the relative phases, reflecting the effects of slight pitching and yawing of the z-stage using the ball-bearing system with the translation. However, the variation width of the relative phases within the small range of z is slightly smaller than that in Fig. 2(a). This comparison suggests that the stage of the air-bearing system is superior to the stage of the ball-bearing system in straightness. However, the variation width of the relative phases within the small range of z is smaller in the ball-bearing system, apparently because the control of the stage by compressed air lacks mechanical stability. The straightness of the z stage in the newest system was estimated to be 3×10^{-7} rad/mm by the Hewlett Packard ultra-high precision laser measurement system; that of the air-bearing system was better than 1×10^{-7} rad/mm [5].

The newest system also accurately positions the z stage with a resolution of 10 nm using a semiconductor laser interferometer (LMD100, Olympus Optical Industry Co., Tokyo, Japan). Though this is inferior in terms of resolution and stability to the He-Ne laser interferometer used in the previous system [5], it achieves sufficient measurement accuracy at a relatively low cost. A network/spectrum analyzer (Model HP-4395A, Hewlett-Packard Co.) was used as the receiver for complex measurements, and a spectrum analyzer (Model HP-8568B, Hewlett-Packard Co.) was used for amplitude measurements. Other electrical circuits are basically the same as those stated in the literature [5]. Though $V(z)$ curves can be measured as either amplitude type or complex type, the measurement of the amplitude-type $V(z)$ curve was adopted basically because of its greater reproducibility. As a result, a resolution in V_{LSAW} measurements at an arbitrary single chosen point on the surface of the specimen was improved to $\pm 0.0013\%$ ($\pm 2\sigma, \sigma$ is the standard deviation) in this system, compared to $\pm 0.002\%$ in the previous system. In addition, a resolution of $\pm 0.003\%$ was achieved within a two-dimensional, continuous-scanning area of 75 mm × 75 mm. The absolute accuracy of the acoustic velocities af-

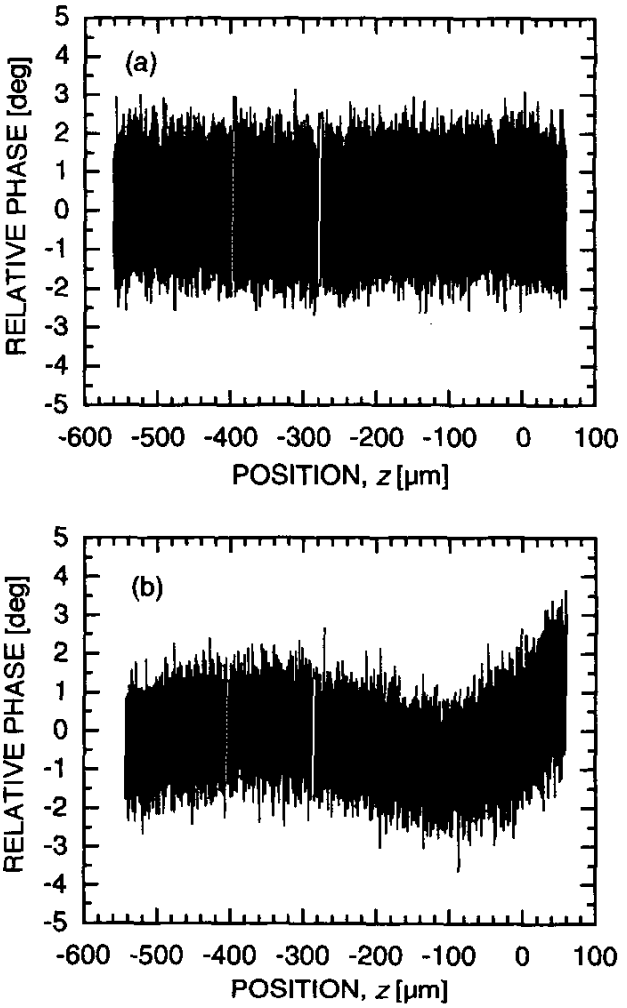

Fig. 2. Relative phase variations of the z-stages with translation detected by the phase measurement using ultrasonic plane waves at 200 MHz. (a) Air bearing; (b) ball bearing.

TABLE I
CURIE TEMPERATURE T_C FOR $LiTaO_3$ SINGLE CRYSTALS PRODUCED AND MEASURED BY MANUFACTURER A.

	T_C[°C]	
Crystal No.	Top	Bottom
A-1	603.2	604.0
A-2	603.9	604.8
A-3	604.7	605.8

TABLE II
CURIE TEMPERATURE T_C FOR $LiTaO_3$ SINGLE CRYSTALS PRODUCED AND MEASURED BY MANUFACTURER B.

Crystal No.	T_C[°C] (Bottom)
B-1	604.4
B-2	608.1
B-3	611.0

ter system calibration using the standard specimen was around ±0.01% [26], [27].

IV. EXPERIMENTS

A. Specimens

The 42°YX-$LiTaO_3$ wafers produced by three manufacturers (A, B, and C) were taken as specimens. The crystals were grown by the Czochralski method. Manufacturers A and B evaluate the crystals by measuring T_C, while manufacturer C does so by measuring a. A total of six wafer substrates taken from the top and bottom of three crystals with different T_C were prepared as the specimens of manufacturer A; a total of six wafer substrates, two wafers from each crystal, taken at arbitrary positions from three crystals with significantly different T_C, were prepared as the specimens of manufacturer B; and a total of 20 wafer substrates, taken from the top and bottom of five crystals with different a were prepared as the specimens of manufacturer C. The T_C and a were measured by the respective manufacturers. Each substrate was about 0.35-mm thick. The diameter of each substrate made by manufacturers A and B was 76 mm; that made by manufacturer C was 100 mm. Detailed values of T_C and a for the specimens are shown in Tables I to III. The T_C for the specimens of manufacturer A was measured both at the top and bottom of the crystals; T_C of manufacturer B and a of manufacturer C were measured for the remaining materials at the bottom of the crystals after the slicing process.

B. Measurements

The velocities of LSAWs propagating along the crystallographic X axis were measured for all the wafer specimens at five measurement points positioned at intervals of 10 mm over a range of ±20 mm in the diameter direction parallel to the X axis. Serious effects of the waves reflected from the back surface of the specimen could be observed because of the thickness (0.35 mm) of the specimens. Therefore, we obtained measured values after removing the effects of reflections from the back surface by applying the moving average processing to the frequency dependence of V_{LSAW} measured at 0.5-MHz steps over a range of 215 to 235 MHz [28] and performing additional system calibration [26].

TABLE III
LATTICE CONSTANT a FOR $LiTaO_3$ SINGLE CRYSTALS PRODUCED AND MEASURED BY MANUFACTURER C.

Crystal No.	a [nm] (Bottom)
C-1	0.515379
C-2	0.515381
C-3	0.515384
C-4	0.515386
C-5	0.515390

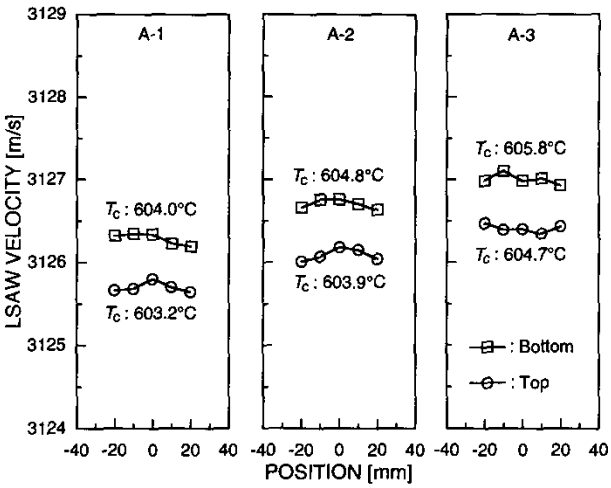

Fig. 3. LSAW velocity distributions for 42°YX-$LiTaO_3$ wafers prepared from three ingots produced by manufacturer A.

Fig. 3 shows the results of the V_{LSAW} distributions measured on the wafers made by manufacturer A. The velocities vary slightly with the positions, and the variations on the wafers were 0.13 to 0.18 m/s. The substrates on the bottom sides of all the crystals tended to have higher V_{LSAW} and T_C than those for the substrates on the top sides. In addition, V_{LSAW} increased as T_C rose.

Fig. 4 shows the V_{LSAW} distributions measured on wafers made by manufacturer B. The profiles of all the wafers except the B-3 No. 2 specimen were very flat, and the V_{LSAW} variations on the wafers were within 0.1 m/s. The V_{LSAW} variation on the B-3 No. 2 specimen was 0.23 m/s. For these wafers, V_{LSAW} increased as T_C rose.

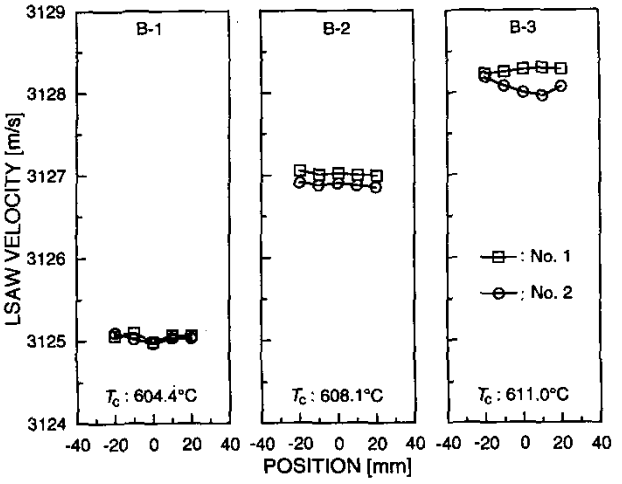

Fig. 4. LSAW velocity distributions for 42°YX-$LiTaO_3$ wafers prepared from three ingots produced by manufacturer B.

Fig. 5 shows the V_{LSAW} distributions measured on the wafers made by manufacturer C. In each crystal, the differences in V_{LSAW} between any two adjacent substrates on the top and bottom sides were very small, with substrates exhibiting similar profiles. The V_{LSAW} variations measured on the wafers were 0.07 to 0.32 m/s. The substrates on the bottom sides of all the crystals tended to have higher V_{LSAW} than the substrates on the top sides. An examination of the relationships of V_{LSAW} with a indicates a trend wherein V_{LSAW} decreases as a increases, and the differences in V_{LSAW} between the substrates on the top and bottom sides become smaller.

C. Relationship between Curie Temperature and LSAW Velocity

Fig. 6 shows the relationship between the T_C data in crystals made by manufacturers A and B and the average values of V_{LSAW} measured at five points on each wafer. These suggest that V_{LSAW} increases as T_C rises. When an approximated straight line is drawn for each set of the results for manufacturers A and B, the gradients of the two lines are almost equal, 1.92°C/(m/s) for manufacturer A and 2.09°C/(m/s) for manufacturer B. The T_C of manufacturer B was measured to be about 2°C higher. This is probably due to some differences in the instruments, methods, and conditions for measuring T_C between manufacturers A and B. We have no information on the exact wafer positions in the crystal boules of manufacturer B; therefore, some errors for T_C should exist due to the different measurement positions in the ingots. In contrast, for the wafers made by manufacturer A, we know that the positions of wafers used for V_{LSAW} measurements are next to the measurement point of T_C, so the errors due to the different measurement positions are negligible.

The relationship between T_C and V_{LSAW} for 42°YX $LiTaO_3$ can be determined as 1.70°C/(m/s) using the relationship between the Li_2O contents $M(Li_2O)$ and V_{LSAW} for 42°YX $LiTaO_3$ calculated in Fig. 1(a), 22.8 (LSAW-m/s)/mol%, and the relationship between T_C and $M(Li_2O)$ in the literature [29]. This result is slightly smaller than the results obtained in Fig. 6 for manufacturers A and B. However, the T_C range of 11.9°C that is used to obtain the approximated straight line is broader than those of 2.6°C for manufacturer A and 6.6°C for manufacturer B. The result of the gradient obtained for the broader range has higher reliability, when considering the measurement errors of about ±1°C for T_C. Therefore, we adopt 1.70°C/(m/s) as the relationship between T_C and V_{LSAW} for 42°YX $LiTaO_3$.

D. Relationship between Lattice Constant and LSAW Velocity

Fig. 7 shows the relationship between a measured by manufacturer C and the measured average values of V_{LSAW}. The V_{LSAW} decreases as a increases. The approximated straight line obtained by the least-squares method for the results on the top sides (circles) is denoted by a dotted line, and that for the results on the bottom sides (dots), by a solid line. The gradients of the two straight lines are -9.76×10^{-6} nm/(m/s) for the dotted line and -7.02×10^{-6} nm/(m/s) for the solid line, corresponding to the differences in V_{LSAW} at the top and bottom positions of the ingots. Thus, it is clear that the lattice constant of $a = 0.515379$ nm for the crystal C-1 might not be measured properly, reflecting some problems in the measuring conditions and accuracy with the X-ray diffractometer system used for the measurements, as the measurement accuracy of V_{LSAW} is ±0.1 m/s or less. We adopted the approximated line for the wafer on the bottom side (solid line) as the lattice constants a were measured in the remaining materials located near the bottom wafer substrate after the slicing process. As a result, -7.02×10^{-6} nm/(m/s) was obtained as the relationship between a and V_{LSAW} for 42°YX $LiTaO_3$.

E. Relationships among Chemical and Physical Characteristics

Table IV summarizes the previously obtained relationships among V_{LSAW} for 42°YX $LiTaO_3$, T_C, and a, in addition to the relationships between V_{LSAW} and $M(Li_2O)$ obtained in Section II and between V_{LSAW} and V_{SAW}. All the characteristics were linearly interrelated to each other. Using the conversion coefficients among those characteristic parameters, we easily can convert from one of the chemical and physical characteristics to any other characteristics for crystal evaluation with a desired parameter. Using the results in Table IV and the relative accuracy of V_{LSAW} measurements, ±0.0013%, corresponding to ±0.04 m/s around 3125 m/s, we can estimate the resolutions of this ultrasonic method for the chemical and physical prop-

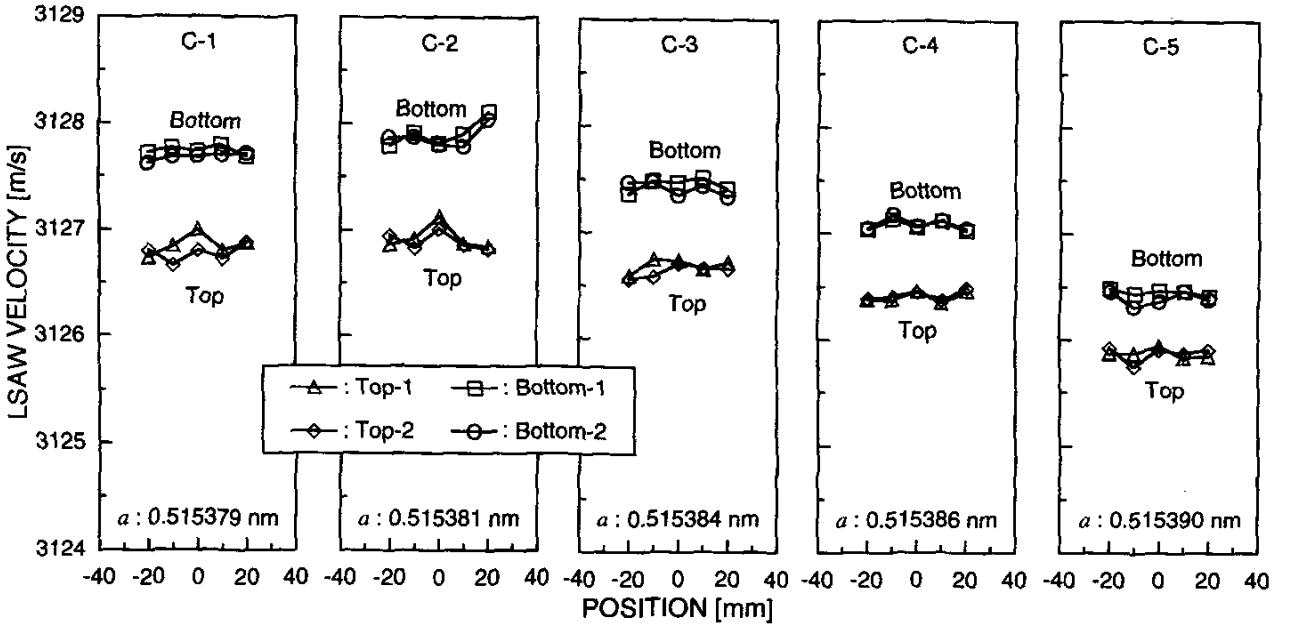

Fig. 5. LSAW velocity distributions for 42°YX-$LiTaO_3$ wafers prepared from five ingots produced by manufacturer C.

TABLE IV
INTERRELATIONSHIPS* AMONG CHEMICAL AND PHYSICAL PROPERTIES FOR 42°YX-$LiTaO_3$ SINGLE CRYSTALS.

		Property (X)				
		V_{LSAW} [m/s]	T_C [°C]	a [nm]	$M(Li_2O)$ [mol%]	V_{SAW} [m/s]
Property (Y)	V_{LSAW} [m/s]	—	1.70	-7.02×10^{-6}	0.0439	1.85
	T_C [°C]	0.588	—	-4.13×10^{-6}	0.0258	1.09
	a [nm]	-0.142×10^{6}	-0.242×10^{6}	—	-0.00625×10^{6}	-0.263×10^{6}
	$M(Li_2O)$ [mol%]	22.8	38.7	-160×10^{-6}	—	42.1
	V_{SAW} [m/s]	0.540	0.919	-3.80×10^{-6}	0.0237	—

*Conversion coefficient for X/Y.

erties of 42°YX-$LiTaO_3$ crystals, as shown in Table V. The resolution in V_{LSAW} is much higher than those in the T_C and a measurements.

V. DISCUSSION

A. Evaluation of Crystals from Different Manufacturers

The measured results of the V_{LSAW} distributions for the wafers obtained from different manufacturers shown in Figs. 3–5 are summarized in Table VI, in order to evaluate homogeneities and inhomogeneities on wafers, in ingots, and among wafers. The variations for the Li_2O contents $M(Li_2O)$ and V_{SAW} converted from the V_{LSAW} variations also are shown in Table VI, based on the relationships presented in Table IV. The V_{LSAW} variations for each of the wafers are within about 0.3 m/s, which corresponds to the V_{SAW} variations within about 0.6 m/s. The V_{LSAW} variations in ingots are about 0.6 m/s maximum for manufacturer A, but are larger for manufacturer C (about 1 m/s maximum). The maximum variations in V_{LSAW} among all of the wafers are 1.30 m/s for manufacturer A and 2.03 m/s for manufacturer C. The converted variations of V_{SAW} are 2.41 m/s for manufacturer A and 3.76 m/s for manufacturer C. We examined the wafers made by manufacturer B here to compare T_C with those for wafers from manufacturer A. However, these specimens are from a wide range of T_C provided for preparation of a more accurate calibration line, so they are excluded from the discussion. If we assume that a tolerance of ±0.04% is adopted for the SAW velocities [30], it would correspond to a tolerance of ±1.69 m/s for SH-type V_{SAW} for 42°YX-$LiTaO_3$ wafers. The distributions on wafers and in ingots from different manufacturers and the distributions among wafers made by manufacturer A are within the tolerance, but the distributions among wafers made by manufacturer C exceed this tolerance.

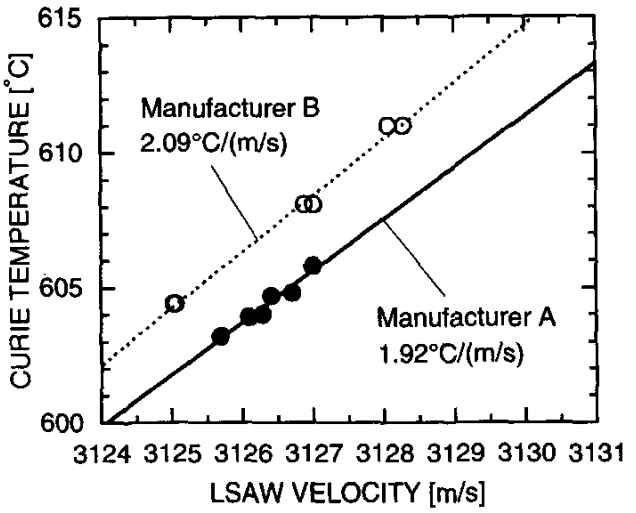

Fig. 6. Measured relationship between LSAW velocity and Curie temperature T_C for 42°YX-$LiTaO_3$ wafers.

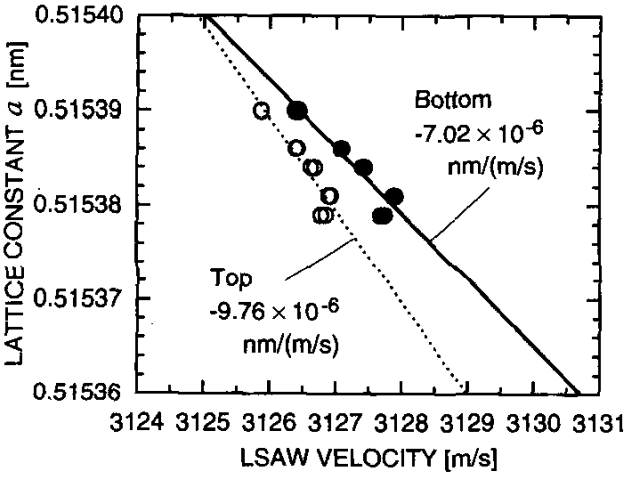

Fig. 7. Measured relationship between LSAW velocity and lattice constant a for 42°YX-$LiTaO_3$ wafers.

TABLE V
RESOLUTIONS OF Li_2O CONTENT, CURIE TEMPERATURE, LATTICE CONSTANT, AND SAW VELOCITY FOR 42°YX-$LiTaO_3$ BY LSAW VELOCITY MEASUREMENTS.

	Resolution
LSAW velocity	±0.04 m/s
Li_2O content	±0.002 mol%
Curie temperature	±0.07°C
Lattice constant a	$\pm 0.3 \times 10^{-6}$ nm
SAW velocity	±0.08 m/s

TABLE VI
VARIATIONS OF MEASURED LSAW VELOCITIES AND OF ESTIMATED Li_2O CONTENTS AND SAW VELOCITIES FOR 42°YX-$LiTaO_3$ WAFERS.

		V_{LSAW} [m/s]	$M(Li_2O)$ [mol%]	V_{SAW} [m/s]
On wafers	A	0.13 ~ 0.18	0.006 ~ 0.008	0.23 ~ 0.33
	B	0.06 ~ 0.23	0.003 ~ 0.010	0.11 ~ 0.42
	C	0.07 ~ 0.32	0.003 ~ 0.014	0.14 ~ 0.59
In ingots	A	0.59 ~ 0.61	0.026 ~ 0.027	1.09 ~ 1.14
	B	—	—	—
	C	0.58 ~ 1.01	0.025 ~ 0.044	1.07 ~ 1.87
Among wafers	A	1.30	0.057	2.41
	B	(3.24)	(0.142)	(6.00)
	C	2.03	0.089	3.76

The V_{LSAW} in ingots made by manufacturers A and C increased from the top to the bottom of the crystals, as shown in Figs. 3 and 5. The relationship between V_{LSAW} and $M(Li_2O)$, 22.8 (LSAW-m/s)/mol%, indicates that $M(Li_2O)$ increases from the top to the bottom of the crystals. The increment of $M(Li_2O)$ is estimated to be 0.026 to 0.027 mol% for manufacturer A and 0.025 to 0.044 mol% for Manufacturer C. The literature [13] reported that $M(Li_2O)$ increased from the top to the bottom of crystals when the chemical composition of the starting material was Li-richer than the congruent composition. This implies that commercial crystals made by both manufacturers A and C were grown with the chemical composition of the starting material slightly Li-richer than the congruent composition.

B. Problems in Evaluating Crystals

1. Comparisons of Tolerances: Manufacturers currently use different methods to evaluate $LiTaO_3$ crystals; most manufacturers use the T_C measurements, but some use the a measurements. Furthermore, independent tolerances are adopted for individual evaluation properties. For example, Table VII shows the tolerances for individual properties for evaluating $LiTaO_3$ crystals. Tolerances of ±3°C for T_C and ±0.00002 nm for a are provided [31]. So far, there have been no examples of standardized comparisons between them, and at present neither manufacturers nor users know which tolerance is broader.

Therefore, based on the results in Table IV, we compared the T_C tolerance of ±3°C and the a tolerance of ±0.00002 nm on the same scale through V_{LSAW} and V_{SAW}. Table VII shows the results of the comparisons. The corresponding tolerances for T_C and a expressed as changes in V_{LSAW} were estimated to be ±1.76 m/s for T_C and ±2.85 m/s for a, and ±3.27 m/s for T_C and ±5.27 m/s for a when expressed as changes in V_{SAW}. These results reveal that the a tolerance is 1.6 times as large as the T_C tolerance. Thus, the differences in tolerance between individual evaluation properties could lower the device yield for

TABLE VII
TOLERANCES FOR LATTICE CONSTANT a AND CURIE TEMPERATURE T_C OF $LiTaO_3$ SINGLE CRYSTALS AND THEIR CORRESPONDING VARIATIONS OF LSAW AND SAW VELOCITIES.

			Corresponding distribution	
Manufacturer	Property	Tolerance	V_{LSAW} [m/s]	V_{SAW} [m/s]
A, B	T_C [°C]	±3	±1.76	±3.27
C	a [nm]	$\pm 20 \times 10^{-6}$	±2.85	±5.27

users who adopt crystals supplied by manufacturers using a larger tolerance, because they would have to manufacture SAW devices using crystals that contain larger variations in V_{SAW} among substrates. Therefore, the tolerances for T_C and a should be equal for the wafer specifications. For example, if a tolerance of ±0.04% is adopted for V_{SAW} [30], the corresponding tolerances can be estimated from the relationships in Table IV as ±1.6°C for T_C, $\pm 6.4 \times 10^{-6}$ nm for a, and ±0.9 m/s for V_{LSAW}.

2. Statistical Comparison of Grown Crystals: Fig. 8 shows accumulated data for some T_C values measured for $LiTaO_3$ crystals grown by manufacturer A and a values measured for crystals grown by manufacturer C during 1999 to 2000. The number of samples n is 1047 for manufacturer A and 436 for manufacturer C. Though manufacturer A measures T_C both at the top and bottom of each crystal ingot, only the results at the bottom are shown here to compare the results with those for a by manufacturer C. The results in Fig. 8 indicate that an average value of T_C for the $LiTaO_3$ crystals produced by manufacturer A is 603.3°C with a standard deviation of 1.0°C, an average value of a for crystals produced by manufacturer C is 0.515382 nm with a standard deviation of 0.000004 nm. To compare the distributions in chemical composition ratio for the two manufacturers, we converted T_C and a in Fig. 8 into V_{LSAW} values as shown in Fig. 9. The results reveal that the average values of V_{LSAW} are 3125.78 m/s for manufacturer A and 3127.62 m/s for manufacturer C, and the average value for manufacturer A is 1.84 m/s smaller than that for manufacturer C. Furthermore, the standard deviations are 0.54 m/s for manufacturer A and 0.57 m/s for manufacturer C, so both are almost the same standard deviations in statistical data. However, Fig. 9 also indicates that the maximum differences of the LSAW velocities are 2.82 m/s for manufacturer A and 5.27 m/s for manufacturer C, so the maximum deviation for manufacturer C is larger. This is because the a tolerance for manufacturer C is larger than the T_C tolerance for manufacturer A, as shown in Table VII.

This discussion has been based on the measured results at the bottoms of the crystal ingots. However, it is necessary in practice to also consider the properties of the wafers at the top positions of the crystals because an erroneous evaluation would be made if there were a distribution of V_{LSAW} or a within a crystal, as shown in Fig. 7. The T_C also was measured at the top positions of crystals for manufacturer A, so we can obtain the statistical distributions of V_{LSAW} converted from the measured values of T_C at the top sides of the $LiTaO_3$ crystals made by manufacturer A, as shown in Fig. 10(a). However, we have no data of a at the top positions of the crystals made by manufacturer C, but we can estimate V_{LSAW} at the top side for a crystal ingot with a measured at the bottom side from the experimental results in Fig. 7. In Fig. 7, the distances along the horizontal axis between the two approximated straight lines represent the differences in V_{LSAW} between the top and bottom sides of the crystals. For example, at the point where $a = 0.51538$ nm, the V_{LSAW} difference can be estimated to be 1 m/s. Thus, we can obtain statistical distributions of V_{LSAW} at the top sides of the crystals made by manufacturer C from values measured at the bottom sides in Fig. 9(b), as shown in Fig. 10(b). The results for manufacturer A shown in Fig. 10(a) present an average V_{LSAW} of 3125.52 m/s with a standard deviation of 0.50 m/s. These results are smaller than the results for the bottom sides, shown in Fig. 9(a), by 0.26 m/s in average value and 0.04 m/s in standard deviation. The results for manufacturer C shown in Fig. 10(b) include an average V_{LSAW} of 3126.76 m/s with a standard deviation of 0.41 m/s. These results are smaller than the results for the bottom, shown in Fig. 9(b), by 0.85 m/s in average and 0.16 m/s in standard deviation. These results thus reveal that the distributions are statistically smaller at the top of the crystals than at the bottom, and, in average, the distributions for $LiTaO_3$ crystals made by manufacturer C are approximately three times larger than those made by manufacturer A. Furthermore, we can see the different chemical compositions of the starting materials between the two manufacturers from the result of the difference in average V_{LSAW} value of 1.24 m/s, corresponding to 0.055 mol% for the Li_2O content.

In contrast, the maximum differences of V_{LSAW} obtained by combining the results in Figs. 9 and 10 are 3.13 m/s for manufacturer A and 5.43 m/s for manufacturer C. Thus, the maximum deviation for manufacturer C is larger, in correspondence to the tolerance shown in Table VII. The above results suggest that, because manufacturer A is growing a larger number of crystals that have a nearly congruent composition and their tolerance is narrower than that for manufacturer C, manufacturer A supplies crystals and wafer substrates with smaller variations in chemical and physical characteristics among the crystals.

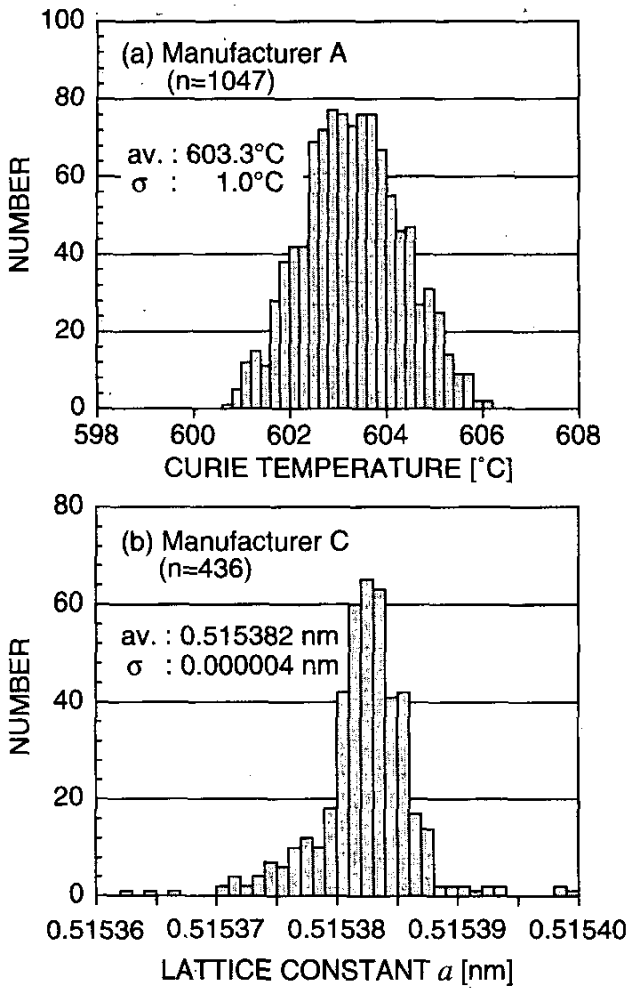

Fig. 8. Statistical distributions of evaluation properties measured for the bottom parts of $LiTaO_3$ crystals grown by two manufacturers. (a) Curie temperature T_C by manufacturer A, (b) Lattice constant a by manufacturer C.

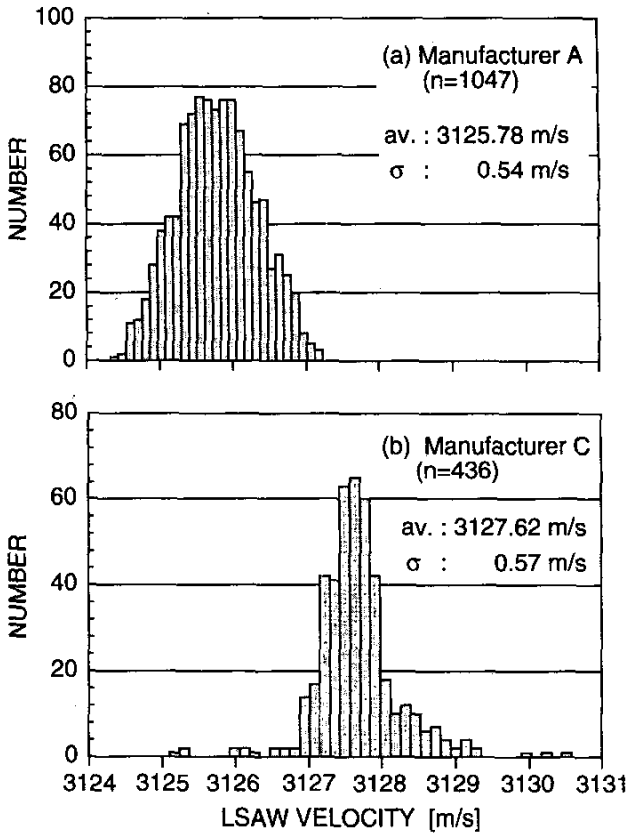

Fig. 9. Statistical distributions of LSAW velocities for the bottom parts of 42°YX-$LiTaO_3$ crystals produced by two manufacturers. The velocities were obtained by the relationships between T_C and V_{LSAW} in Fig. 6 and between a and V_{LSAW} in Fig. 7. (a) Manufacturer A, (b) manufacturer C.

C. Solutions

There are elastic inhomogeneities related to the chemical composition distributions in crystal ingots, as shown in Table VI. Therefore, if T_C or a is measured only at the bottom sides of crystals, for example, as in the case of manufacturer C (Fig. 7), distributions in the crystals cannot be known correctly. In contrast, when T_C or a is measured both at the top and bottom sides of the crystals, as in the case of manufacturer A (Fig. 6), distributions that reflect inhomogeneities in the crystals can be determined. Similar things also are indicated from the results in Figs. 9 and 10. Although the use of higher-resolution techniques is clearly suitable for single crystal evaluation, it is at least necessary to conduct measurements both at the top and bottom sides of crystal ingots. It also is important to present the results to users who design devices, to enable them to fabricate devices with high yield and superior performance.

One way to obtain a successful evaluation based on only the results from one side of the top and bottom of crystals is to grow more homogeneous crystals with the proper congruent composition useful for successive crystal production. As stated in IV.B; the crystals made by manufacturer A have an average difference of 0.26 m/s in V_{LSAW} between the top and bottom sides of the crystals, the difference in the crystals made by manufacturer C was 0.85 m/s. Thus, manufacturer A is growing a larger number of crystals that have nearly congruent compositions. The congruent composition estimated from the present results lies around the intersection of the solid line and dotted line in Fig. 7 (a = 0.51540 nm). If a = 0.51540 nm, V_{LSAW} is 3124.6 m/s, corresponding to 601.0°C for T_C. However, because the relationship between V_{LSAW} and T_C used here was obtained from the T_C values measured in manufacturer A and, as shown in Fig. 6, it also involves some problems with absolute accuracy due to the measuring instruments and conditions used for T_C measurements by manufacturer A, so this is not always the absolute value to yield a congruent composition. This also may apply to a. In any case, adopting the growth conditions that achieve around 0.51540 nm for a in the current production line would be one way for manufacturer C to grow more ho-

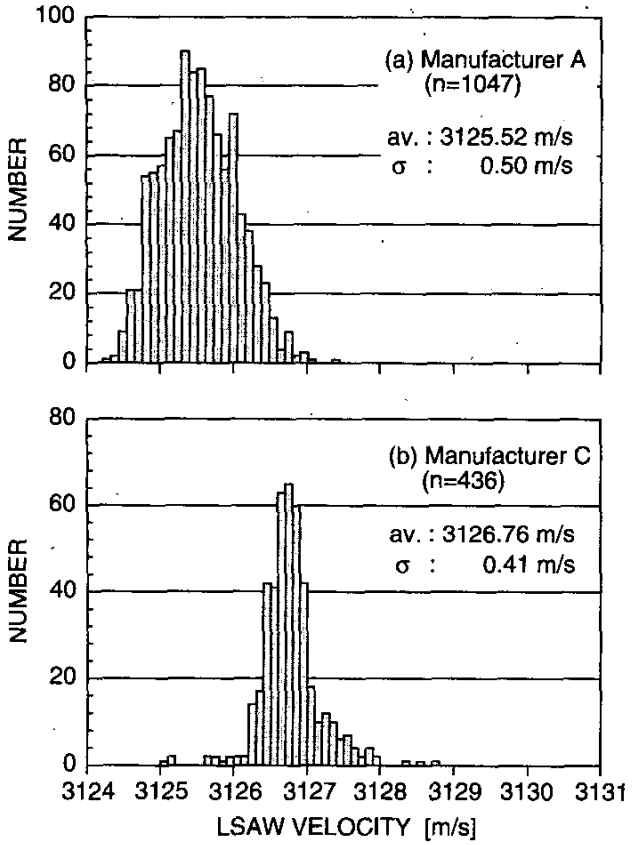

Fig. 10. Statistical distributions of LSAW velocities for the top parts of 42°YX-$LiTaO_3$ single crystals produced by two manufacturers. The velocities for manufacturer A were obtained by the relationships between T_C and V_{LSAW} in Fig. 6, and those for manufacturer C were estimated using the results of Fig. 7. (a) Manfacturer A, (b) manufacturer C.

mogeneous crystals. Similarly, it would be advantageous for manufacturer A to adopt the growth conditions that achieve around 601.0°C for T_C. It is possible to grow more homogeneous crystals by feeding the measurement results of V_{LSAW} back to the crystal growth conditions, particularly to the chemical composition of the starting material; a detailed description of this will be presented in another paper.

VI. Conclusions

In this study of evaluating the chemical compositions of $LiTaO_3$ crystals, we implemented a standardized comparison and evaluation of the tolerances for T_C and a, which are determined independently by individual manufacturers, through the Rayleigh-type V_{LSAW} measured by the LFB-UMC system.

We first measured V_{LSAW} for 42°YX-$LiTaO_3$ wafers obtained from three crystal manufacturers, and then experimentally obtained the relationship between T_C and a measured by the individual manufacturers. The relationship between V_{LSAW} and V_{SAW} for 42°YX-$LiTaO_3$ wafers was obtained through numerical calculations based on the chemical composition dependences of the acoustical physical constants of $LiTaO_3$ crystals. The T_C and a can be converted into values of the same parameter (V_{LSAW} or V_{SAW}) using these relationships. As a result, we found that the tolerance for a of ±0.00002 nm is 1.6 times larger than the tolerance for T_C of ±3°C, thus clarifying one problem in the current evaluation methods. However, we suggested serious problems associated with the measuring instruments and conditions for T_C due to which the experimental results revealed a difference of 2°C between the T_C values measured by two individual manufacturers. A standardized tolerance of ±0.04% for V_{SAW} corresponds to the following tolerances for each characteristic value: ±1.6°C for T_C, $\pm 6.4 \times 10^{-6}$ nm for a, and ±0.9 m/s for V_{LSAW}. Using the statistical results of T_C and a for $LiTaO_3$ crystals manufactured by two manufacturers from 1999 to 2000, we evaluated the crystals between the two manufacturers on the same scale of V_{LSAW}. This clarified the differences in V_{LSAW} or chemical composition for average crystal ingots from the two manufacturers as well as the differences in the distributions among crystals that correspond to the tolerances of individual manufacturers.

As described above, some problems in growing and evaluating crystals were clarified by examining the interrelationships among various chemical and physical characteristics using the LFB-UMC system and by evaluating the crystals using the standardized scale of V_{LSAW}. It is at least necessary to perform evaluations at the top and bottom sides of crystals to identify the variations and distributions within the crystals. Furthermore, it is important to feed the evaluation results back to the growth conditions to obtain more homogeneous crystals, and to provide such results for users who fabricate SAW devices. Grown crystals also should be evaluated under standardized criteria to supply crystal substrates with small variations in the physical and chemical characteristics. To that end, we believe that this study will provide an important guideline for standardizing the specifications for wafers. In addition, because the LFB-UMC system can be used to evaluate both Rayleigh-type SAW device materials and SH-type SAW device materials, we consider that this system is an important material evaluation technology that enables superior accuracy and a standardized evaluation of SAW device materials.

Though we evaluated the chemical composition ratio as an essential factor for determining the characteristics of substrate materials in this study, other important problems associated with surface damage of the substrates, which is considered to produce properties differing from the bulk property, were not considered. A damaged surface layer contains disorders introduced to the surface of the substrates during slicing and polishing, such as surface roughness, micro cracks, and anomalous layers. This is a more important problem, particularly for devices for which the key material properties are within 1 μm of the surface, such as SAW devices and surface waveguide-type

optical devices. This influence is particularly significant for SHF-band SAW devices, so it will be necessary in the near future to consider not only the chemical composition problems but also the influence from surface damage to the substrates.

ACKNOWLEDGMENT

The authors are grateful to Y. Ono for his useful advice for the measurements.

REFERENCES

[1] R. M. Hays and C. S. Hartmann, "Surface-acoustic-wave devices for communications," *Proc. IEEE*, vol. 64, pp. 652–671, May 1976.

[2] C. C. W. Ruppel, R. Dill, A. Fischerauer, G. Fischerauer, W. Gawlik, J. Machui, F. Müller, L. Reindl, W. Ruile, G. Scholl, I. Schropp, and K. C. Wagner, "SAW devices for consumer communication applications," *IEEE Trans. Ultrason., Ferroelect., Freq. Contr.*, vol. 40, pp. 438–452, Sep. 1993.

[3] K. Yamanouchi, "Surface acoustic wave devices," *IEICE Trans. Electron.*, vol. J82-C-I, pp. 689–696, Dec. 1999.

[4] J. Kushibiki and N. Chubachi, "Material characterization by line-focus-beam acoustic microscope," *IEEE Trans. Sonics Ultrason.*, vol. SU-32, pp. 189–212, Mar. 1985.

[5] J. Kushibiki, Y. Ono, Y. Ohashi, and M. Arakawa, "Development of the line-focus-beam ultrasonic material characterization system," *IEEE Trans. Ultrason., Ferroelect., Freq. Contr.*, vol. 49, pp. 99–113, Jan. 2002.

[6] J. Kushibiki, H. Asano, T. Ueda, and N. Chubachi, "Application of line-focus-beam acoustic microscope to inhomogeneity detection on SAW device materials," in *Proc. IEEE Ultrason. Symp.*, 1986, pp. 749–753.

[7] J. Kushibiki, H. Takahashi, T. Kobayashi, and N. Chubachi, "Quantitative evaluation of elastic properties of $LiTaO_3$ crystals by line-focus-beam acoustic microscopy," *Appl. Phys. Lett.*, vol. 58, pp. 893–895, Mar. 1991.

[8] J. Kushibiki, H. Takahashi, T. Kobayashi, and N. Chubachi, "Characterization of $LiNbO_3$ crystals by line-focus-beam acoustic microscopy," *Appl. Phys. Lett.*, vol. 58, pp. 2622–2624, June 1991.

[9] J. Kushibiki, T. Kobayashi, H. Ishiji, and N. Chubachi, "Elastic properties of 5-mol% MgO doped $LiNbO_3$ crystals measured by line focus beam acoustic microscopy," *Appl. Phys. Lett.*, vol. 61, pp. 2164–2166, Nov. 1992.

[10] J. Kushibiki, H. Ishiji, T. Kobayashi, N. Chubachi, I. Sahashi, and T. Sasamata, "Characterization of $36°YX$-$LiTaO_3$ wafers by line-focus-beam acoustic microscopy," *IEEE Trans. Ultrason., Ferroelect., Freq. Contr.*, vol. 42, pp. 83–90, Jan. 1995.

[11] J. Kushibiki, T. Kobayashi, H. Ishiji, and C. K. Jen, "Surface-acoustic-wave properties of MgO-doped $LiNbO_3$ single crystals measured by line-focus-beam acoustic microscopy," *J. Appl. Phys.*, vol. 85, pp. 7863–7868, June 1999.

[12] J. Kushibiki, Y. Ono, and I. Takanaga, "Ultrasonic microspectroscopy of $LiNbO_3$ and $LiTaO_3$ single crystals for SAW devices," *IEICE Trans. Electron.*, vol. J82-C-I, pp. 715–727, Dec. 1999.

[13] J. Kushibiki, T. Okuzawa, J. Hirohashi, and Y. Ohashi, "Line-focus-beam acoustic microscopy characterization of optical-grade $LiTaO_3$ single crystals," *J. Appl. Phys.*, vol. 87, pp. 4395–4403, May 2000.

[14] J. Kushibiki, Y. Ohashi, and Y. Ono, "Evaluation and selection of $LiNbO_3$ and $LiTaO_3$ substrates for SAW devices by the LFB ultrasonic material characterization system," *IEEE Trans. Ultrason., Ferroelect., Freq. Contr.*, vol. 47, pp. 1068–1076, July 2000.

[15] K. Shibayama, K. Yamanouchi, H. Sato, and T. Meguro, "Optimum cut for rotated Y-cut $LiNbO_3$ crystal used as the substrate of acoustic-surface-wave filters," *Proc. IEEE*, vol. 64, pp. 595–597, May 1976.

[16] H. Hirano, T. Fukuda, S. Matsumura, and S. Takahashi, "$LiTaO_3$ single crystals for SAW device applications: (1) Characteristics of the material," in *Proc. 1st Meeting on Ferroelectric Materials and Their Applications*, Kyoto, Japan, 1978, pp. 81–86.

[17] K. Nakamura, M. Kazumi, and H. Shimizu, "SH-type and Rayleigh-type surface waves on rotated Y-cut $LiTaO_3$," in *Proc. IEEE Ultrason. Symp.*, 1977, pp. 819–822.

[18] R. M. White and F. W. Voltmer, "Direct piezoelectric coupling to surface elastic waves," *Appl. Phys. Lett.*, vol. 7, pp. 314–316, Dec. 1965.

[19] K. Yamanouchi and K. Shibayama, "Elastic surface-wave excitation, using parallel-line electrodes above piezoelectric plates," *J. Acoust. Soc. Amer.*, vol. 41, pp. 222–223, Jan. 1967.

[20] J. Kushibiki, I. Takanaga, S. Komatsuzaki, and T. Ujiie, "Chemical composition dependences of the acoustical physical constants of $LiNbO_3$ and $LiTaO_3$ single crystals," *J. Appl. Phys.*, to be published.

[21] O. Kawachi, G. Endoh, M. Ueda, O. Ikata, K. Hashimoto, and M. Yamaguchi, "Optimum cut of $LiTaO_3$ for high performance leaky surface acoustic wave filters," in *Proc. IEEE Ultrason. Symp.*, 1996, pp. 71–76.

[22] K. Hashimoto, M. Yamaguchi, S. Mineyoshi, O. Kawachi, M. Ueda, G. Endoh, and O. Ikata, "Optimum leaky-SAW cut of $LiTaO_3$ for minimised insertion loss devices," in *Proc. IEEE Ultrason. Symp.*, 1997, pp. 245–254.

[23] J. J. Campbell and W. R. Jones, "Propagation of surface waves at the boundary between a piezoelectric crystal and a fluid medium," *IEEE Trans. Sonics Ultrason.*, vol. SU-17, pp. 71–76, Apr. 1970.

[24] J. J. Campbell and W. R. Jones, "A method for estimating optimal crystal cuts and propagation directions for excitation of piezoelectric surface waves," *IEEE Trans. Sonics Ultrason.*, vol. SU-15, pp. 209–217, Oct. 1968.

[25] Y. Ono, J. Kushibiki, and N. Chubachi, "A measurement method of moving characteristics of precision mechanical-translation stages using ultrasonic plane waves and its application to a line-focus-beam acoustic microscopy system," *IEICE Trans. Fundamentals*, vol. J78-A, pp. 279–286, Mar. 1995.

[26] J. Kushibiki and M. Arakawa, "A method for calibrating the line-focus-beam acoustic microscopy system," *IEEE Trans. Ultrason., Ferroelect., Freq. Contr.*, vol. 45, pp. 421–430, Mar. 1998.

[27] J. Kushibiki, M. Arakawa, and R. Okabe, "High-accuracy standard specimens for the line-focus-beam ultrasonic material characterization system," *IEEE Trans. Ultrason., Ferroelect., Freq. Contr.*, to be published.

[28] J. Kushibiki, Y. Ohashi, and M. Arakawa, "Influence of reflected waves from the back surface of thin solid-plate specimen on velocity measurements by line-focus-beam acoustic microscopy," *IEEE Trans. Ultrason., Ferroelect., Freq. Contr.*, vol. 47, pp. 274–284, Jan. 2000.

[29] M. Sato, A. Iwama, J. Yamada, M. Hikita, and Y. Furukawa, "SAW velocity variation $LiTaO_3$ substrates," *Jpn. J. Appl. Phys.*, suppl. 28–1, vol. 28, pp. 111–113, 1989.

[30] K. Yamada, T. Omi, S. Matsumura, and T. Nishimura, "Characterization of 4-inch $LiTaO_3$ single crystals for SAW device application," in *Proc. IEEE Ultrason. Symp.*, 1984, pp. 243–248.

[31] *IEC-PAS, "Single crystal wafers applied for surface acoustic wave device: Specification and Measuring Method"*, IEICE/Std-0002, April 17, 2001.

Jun-ichi Kushibiki (M'83) was born in Hirosaki, Japan, on November 23, 1947. He received the B.S., M.S., and Ph.D. degrees in electrical engineering from Tohoku University, Sendai, Japan, in 1971, 1973, and 1976, respectively.

In 1976, he became Research Associate at the Research Institute of Electrical Communication, Tohoku University. In 1979, he joined the Department of Electrical Engineering, Faculty of Engineering, Tohoku University, where he was Associate Professor from

1988 to 1993 and became Professor in 1994. He has been studying ultrasonic metrology, especially acoustic microscopy and its applications, and has established a method of material characterization by LFB acoustic microscopy. He also has been interested in biological tissue characterization in the higher frequency range, applying both bulk and acoustic microscopy techniques.

Dr. Kushibiki is a member of the Acoustical Society of America; the Institute of Electronics, Information, and Communication Engineers of Japan; the Institute of Electrical Engineers of Japan; the Acoustical Society of Japan; and the Japan Society of Ultrasonics in Medicine.

Yuji Ohashi was born in Toyama prefecture, Japan on August 27, 1973. He received the B.S. and M.S. degrees in electrical engineering from Tohoku University, Sendai, Japan in 1996 and 1999, respectively.

He is currently studying toward the Ph.D. degree at Tohoku University. His research interests include development of line-focus-beam acoustic microscopy system and its application to materials characterization.

Mr. Ohashi in a member of the Acoustical Society of Japan.

Takaaki Ujiie was born in Kanazawa, Japan, on October 5, 1976. He received the B.S. and M.S. degrees in electrical engineering from Tohoku University, Sendai, Japan, in 1999 and 2001, respectively. He joined Pioneer Corporation in 2001.